Available online at www.sciencedirect.com
ScienceDirect
Journal of Magnetic Resonance 190 (2008) 154–159
JMR Journal of Magnetic Resonance
www.elsevier.com/locate/jmr

Communication

Post-processing of EPR spectra by convolution filtering: Calculation of a harmonics' series and automatic separation of fast-motion components from spin-label EPR spectra

Alex I. Smirnov *

Department of Chemistry, North Carolina State University, Raleigh, NC 27695-8204, USA

Received 22 July 2007; revised 5 October 2007
Available online 14 October 2007

Abstract

This communication reports on post-processing of continuous wave EPR spectra by a digital convolution with filter functions that are subjected to differentiation or the Kramers–Krönig transform analytically. In case of differentiation, such a procedure improves spectral resolution in the higher harmonics enhancing the relative amplitude of sharp spectral features over the broad lines. At the same time high-frequency noise is suppressed through filtering. These features are illustrated on an example of a Lorentzian filter function that has a principal advantage of adding a known magnitude of homogeneous broadening to the spectral shapes. Such spectral distortion could be easily and accurately accounted for in the consequent least-squares data modeling. Application examples include calculation of higher harmonics from pure absorption echo-detected EPR spectra and resolving small hyperfine coupling that are unnoticeable in conventional first derivative EPR spectra. Another example involves speedy and automatic separation of fast and broad slow-motion components from spin-label EPR spectra without explicit simulation of the slow motion spectrum. The method is illustrated on examples of X-band EPR spectra of partially aggregated membrane peptides.

Keywords: EPR; Data processing; Filtering; Spin-labeling EPR; Data modeling; Membrane peptides

1. Introduction

One common experimental problem of site-directed spin-labeling continuous wave (CW) EPR experiments is the presence of multiple spectral components such as a fast-motion component that would overlap with the rest of the spectrum. The former component could be present for some undesirable reasons related to the sample preparation including residual free label that was not removed by dialysis and/or contamination from a denatured protein. In other studies the balance between the fast motion and immobilized components is of specific interest as an indication of two conformational states. Examples include protein folding and equilibrium between aggregated and monomer viral peptides in lipid bilayers. In both cases accurate separation of spectral components is highly desirable but difficult, especially for only partially resolved lines. The latter often requires rigorous simulations and least-squares optimization of spectral shapes corresponding to multiple species.

It is well-documented that resolution of CW EPR spectroscopy could be improved by the use of higher harmonics detected experimentally by phase-sensitive detection or obtained at the post-processing stage (e.g. see [1] and references therein). One could find the post-processing approach to be more convenient in practice as it does not require any new hardware and can be used for any digitized spectra. For this purpose Hyde and coworkers developed a pseudomodulation—a computer-based strategy for resolution enhancement [1–3]. In brief, this strategy is based on computer simulations of the effect of a sinusoidal magnetic

* Fax: +1 919 513 8909.
E-mail address: Alex_Smirnov@ncsu.edu

1090-7807/$ - see front matter © 2007 Elsevier Inc. All rights reserved.
doi:10.1016/j.jmr.2007.10.006

field modulation on EPR spectra. Modulation amplitude could be varied and higher harmonics are calculated even if only the first harmonic has been originally measured [1]. Subtraction and addition of various amounts of even harmonics to the original spectrum resulted in the resolution enhancement [1]. In their studies Hyde and coworkers arrived to several practical conclusions. Among those was the observation that addition of harmonics greater than the second is not worthwhile as it adds considerable amount of noise.

Indeed, because of noise considerations, only the first harmonics of the resonance signal are typically detected and displayed in CW EPR although second-derivative displays have been used to improve resolution between partially-resolved spectral components of spin probes partitioned between aqueous and hydrocarbon phases of micelles [4]. In some cases echo-detected field-swept EPR spectra are differentiated digitally in order to obtain a more convenient for an EPR spectroscopist first-derivative display (e.g. [5]). Digital differentiation of experimental spectra could be achieved by using the above-mentioned pseudomodulation technique [1] or, by applying various differentiation filters (e.g. see [6] and reference therein).

Although the software for digital differentiation of CW EPR spectra is easily available, literature survey shows that this approach has been rarely employed for calculating harmonics higher than the second. One reason for this is that the digital differentiation enhances high-frequency contributions leading to an increase in noise level. The high-frequency noise could be suppressed by increasing the amplitude of magnetic field modulation (either at the experimental or the post-processing stages) but this comes at the cost of distorting CW EPR line shapes. For first derivative EPR spectra exhibited by spin labels in fast motion limit such distortions could be accurately accounted for through spectral simulations using the model of Robinson and coworkers [7,8]. More recently, Nielsen et al. analyzed resolution-enhancing effects of magnetic field modulation through solving Bloch equations [9]. The Robinson model has been also applied for analyzing EPR oximetry data from probes exhibiting spectra of Lorentzian shape [10,11].

Here another strategy for digital differentiation EPR and other spectroscopic signals is presented. Rather than simulating effects of sinusoidal field modulation, differentiation of digitized spectra is replaced by a convolution with a filter function of a chosen derivative form. Such a procedure improves spectral resolution in the higher harmonics that enhance relative amplitude of sharp spectral features over the broad lines. At the same time raising high-frequency noise is suppressed through filtering. These features are illustrated on an example of a Lorentzian filter function that has a principal advantage of adding a known magnitude of homogeneous broadening to the spectral shapes. Such spectral distortion could be easily and accurately accounted for in the consequent least-squares data modeling. Moreover, existing convolution-based fitting EPR software [12] could be utilized for all the spectral manipulations. Application examples include calculation of higher harmonics from pure absorption echo-detected EPR spectra and resolving small hyperfine coupling that are unnoticeable in conventional first derivative EPR spectra. Another example involves resolving overlapping spin-label EPR spectra from slow (broad) and fast (sharp) spectral components. It is shown that the fast component could be digitally filtered out in a higher harmonic display, least-squares simulated to determine all the parameters, and precisely back-calculated as it should appear in the normal first-derivative display before any filtering. Such a procedure leads to fast and automatic separation of sharp spectral component without explicit simulation of the slow motion spectrum. The method is illustrated on examples of X-band EPR spectra of partially aggregated membrane peptides.

2. Theory and methods

Post-processing of digital signals usually involves filtering that could be easily accomplished in frequency domain by multiplying Fourier transform image $P(\omega)$ of the signal $p(B)$ by a window function $F(\omega)$

$$I(\omega) = P(\omega) \cdot F(\omega) \tag{1}$$

yielding the filtered signal $I(\omega)$. The window $F(\omega)$ could be chosen to suppress undesirable frequencies and/or to select the signals occurring only within specific frequency window [13]. In the field domain Eq. (1) corresponds to a convolution integral

$$I(B) = \int p(B - B')f(B)\mathrm{d}b = p(B) \otimes f(B), \tag{2}$$

where $\otimes$ is the convolution symbol.

One useful property of the convolution integral is that differentiation of the filtered signal $I(B)$ requires taking derivative of only one of the functions in the right-hand part of Eq. (2)

$$I'(B) = p'(B) \otimes f(B) = p(B) \otimes f'(B). \tag{3}$$

Thus, instead of differentiating the signal $p(B)$ and then filtering the noise one could differentiate the filter function $f(B)$ instead. Advantage of the latter is that such a differentiation could be easily carried for the filter function in the analytical form.

While many filter functions $f(B)$ could be applied for differentiation of EPR spectra using Eq. (3), let us consider the case of a Lorentzian filter

$$f(B) = \frac{2A}{\pi} \frac{\Delta B_{1/2}^2}{\Delta B_{1/2}^2 + 4(B_0 - B)^2}, \tag{4}$$

where A is the value of the Lorentzian line integral, B_0 is the center of the line, and $\Delta B_{1/2}$ is the width at half-height. It is easy to show that convolution of two Lorentzian functions $f_1(B)$ and $f_2(B)$ with corresponding widths $\Delta B_{1,1/2}$ and $\Delta B_{2,1/2}$ yields a Lorentzian function with width

$\Delta B_{1/2} = \Delta B_{1,1/2} + \Delta B_{2,1/2}$. Thus, the only spectral distortion caused by application of a Lorentzian filter would be an additional homogeneous broadening of $\Delta B_{1/2}$ in magnitude. Such a broadening could be easily accounted for during least-squares simulations as all CW EPR spectra contain some amount of homogeneous broadening.

One could also calculate higher harmonics of EPR spectra with help of convolution filtering

$$\frac{\partial^n I(B)}{\partial B^n} = p(B) \otimes \frac{\partial^n f(B)}{\partial B^n}. \quad (5)$$

Again, calculations are simplified and accuracy is improved if higher derivatives of the filter functions are derived analytically.

The properties of the filter function in Eqs. (3) or (5) could be also adjusted depending upon experimental needs. Higher harmonics are usually employed in EPR to improve the spectral resolution by sharpening the lines and emphasizing high-frequency signal components [2–4]. Indeed, differentiation in the field domain is equivalent to multiplication by $|\omega|$ in the frequency domain [13]. When applied n-times, such a procedure eliminates polynomial contributions of up to $(n-1)$ order, thus, effectively emphasizing high-frequency components and virtually eliminating broad lines. However, the major drawback of using higher harmonics lays in an increase of high-frequency noise. The noise level could be somewhat attenuated by increasing the filter width but this comes at the cost of spectral resolution. One may also want to adjust the filter width for each of the harmonics.

Convolution-based filtered differentiation given by Eq. (3) could be applied sequentially producing a series of harmonics. For Lorentzian filter of the width $\Delta B_{1/2}$ this sequential differentiation would produce a cumulative effect: each next harmonic in the sequence will contain additional $\Delta B_{1/2}$ homogeneous broadening with respect to the previous member of the series. In other words, after n-differentiations the final spectrum will be broadened by $n\Delta B_{1/2}$.

Another useful feature of Eq. (5) is that least-squares simulations of higher harmonics obtained this way would require only modest modification of the existing programs as the spectral shape $p(B)$ represents a conventional EPR display. Once a model function for $p(B)$ is calculated, the convolution integral Eq. (5) could be evaluated digitally using efficient fast Fourier transform (FFT) algorithms and compared with filtered high harmonic $I(B)$. Convolution-based fitting for EPR spectra has been described in the past [12] and has shown to be very effective for several spin-labeling EPR applications [14–16].

It is worthwhile to note here that some other spectral transformations, such as, for example, Kramers–Krönig transform, T_{KK}, for calculating out-of-phase component could be also carried out by convolution filtering

$$T_{KK}(I(B)) = p(B) \otimes T_{KK}(f(B)). \quad (6)$$

Similar to differentiation, instead of digitally calculating Kramers–Krönig transform directly from the experimental spectrum, the filter function is subjected to this transformation instead. If this latter could be carried out analytically, the only remaining step will be a digital convolution that could be carried out by a FFT algorithm.

3. Results and discussion

3.1. Calculation of higher harmonics and dispersion signals from absorption EPR spectra

To demonstrate the use of Eq. (3) for differentiating absorption EPR spectra, a Lorentzian filter was applied to calculate the first and the second absorption harmonics as well as the first dispersion harmonic from an echo-detected pure absorption spectrum. 130 GHz rigid-limit ($T = 25$ K) EPR spectrum from a solution 5-doxyl stearic acid in deuterated 2-propanol-d1. The spectrum was digitized to 800 data points over 400 G and reported in ref. [17]. The first harmonic absorption spectrum (Fig. 1B) was calculated by convolving the original spectrum (A) with a first-derivative Lorentzian filter of 1.5 G (or three data point intervals) in peak-to-peak width. Consecutive application of the same filter yielded the second derivative absorption display (C). Note that while the presence of the two g_x components with positions marked by dashed lines is hardly noticeable in the original absorption spectrum (A), it becomes evident in the first and the second-derivative displays (B, C). The nature of the two g_x components is discussed in ref. [17].

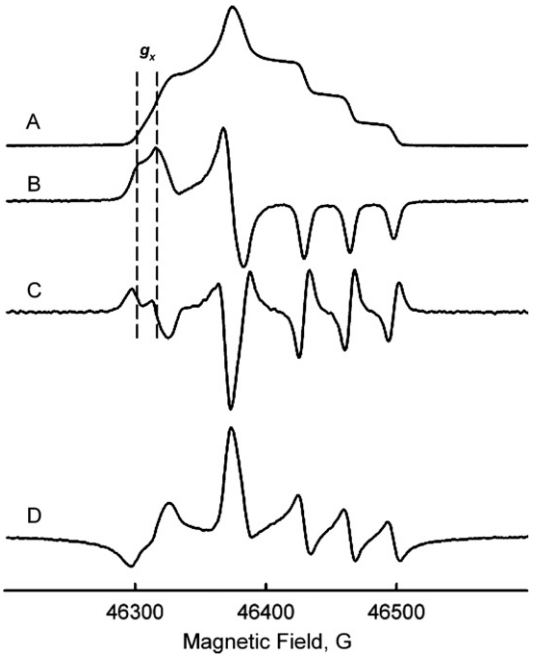

Fig. 1. Experimental echo-detected absorption rigid-limit 130 GHz EPR spectrum from 5-doxyl stearic acid in deuterated 2-propanol-d1 (A) and other spectral displays obtained through post-processing using a Lorentzian filter and Eq. (3): the first (B) and the second (C) harmonic absorption and first harmonic dispersion (D) spectra. All spectra are normalized by the peak-to-peak amplitude. Dashed lines mark positions of the two g_x components. See text for further details.

Convolution of the original spectrum (Fig. 1A) with a first-derivative Lorentzian filter already subjected to the Kramers–Krönig transform yielded the first-derivative dispersion display (C). Again, this transformation has been carried out by a FFT convolution of the experimental with a well-known analytical expression for the dispersive Lorentzian shape.

3.2. Determination of unresolved hyperfine coupling constants from high harmonics of CW EPR spectra

Small hyperfine couplings are often unresolved in CW EPR spectra of organic free radicals and, therefore, are commonly determined from ENDOR and/or NMR experiments [18,19]. The positively charged nitroxide spin label, 2,2,6,6-tetramethyl-piperidine-*N*-oxyl-4-trimethyl-ammonium (Cat1), is one example of such a radical.

Fig. 2A shows a low-field nitrogen hyperfine component of an EPR spectrum from 1 mM aqueous solution of (Cat1) at 297 K (A) and a series of harmonics (B–E) generated using a Lorentzian filter of two data intervals (or 48.8 mG) in width applied sequentially. While the presence of proton hyperfine structure is virtually unnoticeable in the original. spectrum (A), the fourth (D) and the fifth (E) harmonics exhibit well-resolved hyperfine patterns, although with a decreased signal-to-noise ratio.

Fig. 3 illustrates the effect of the Lorentzian filter width on the fifth harmonic of the low-field nitrogen hyperfine component of Cat1 the EPR spectrum: increasing the filter width decreases the high-frequency noise but also decreases the resolution. The latter becomes evident from somewhat suppressed line intensities of the spectrum (C) vs. (B).

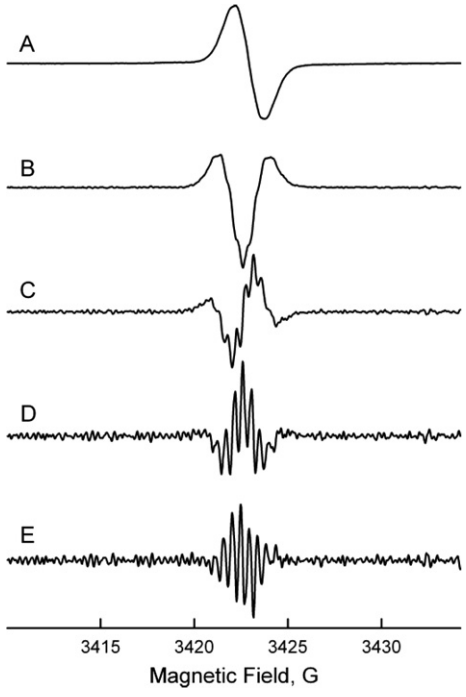

Fig. 2. A low-field nitrogen hyperfine component of an experimental X-band (9.5 GHz) spectrum of 1 mM aqueous solution of 2,2,6,6-tetramethyl-piperidine-*N*-oxyl-4-trimethyl-ammonium (Cat1) at 297 K (A) and a series of harmonics (B–E) generated using a Lorentzian filter of two data intervals (or 48.8 mG) in peak-to-peak width applied sequentially. All spectra are normalized by the peak-to-peak amplitude and contain 1024 data points.

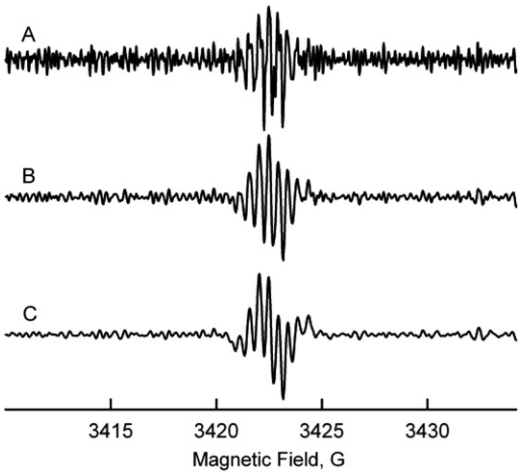

Fig. 3. Effects of the Lorentzian filter width on the fifth harmonic of the low-field nitrogen hyperfine component of the Cat1 EPR spectrum. Cumulative homogeneous (Lorentzian) peak-to-peak broadening of (A) is four data point intervals (97.7 mG), (B) 8 intervals (195.4 mG), (C) 12 intervals (293.1 mG). All spectra are normalized by the peak-to-peak amplitude and digitized to 1024 data points.

The fourth or the fifth harmonics of the Cat1 EPR spectrum could be used to determine proton hyperfine coupling constants through least-squares simulations (Fig. 4). Such simulations have been carried out using EWVoigt program described previously [12]. This program simulates fast motion EPR spectra in either first derivative or an integral form and accounts for a Gaussian broadening. In order to generate higher harmonics the results of the simulations were convolved with an additional Lorentzian function that was derived analytically for the corresponding harmonic. The Lorentzian width was set exactly to the cumulative broadening of differentiated spectrum for which the filter with the peak-to-peak width of three data intervals or 73.2 mG was applied sequentially. The results of simultaneous fitting of the fourth and the fifth harmonics are shown in Fig. 4. Residuals of the fit—differences between the "experimental" and the simulated spectra (B and D)—show no systematic deviations between the data and the model. The splitting on the 6 equivalent protons was determined to be $a_{H1}(6) = 477 \pm 1$ mG and $a_{H2}(2) = 298 \pm 1$ mG for the two equivalent protons ($T = 297$ K). These data are similar to $a_{H1}(6) = 425 \pm 12$ mG and $a_{H2}(2) = 300 \pm 30$ mG measured by NMR at $T = 370$ K for saturated solution of a similar nitroxide Cat12 [19].

Once proton hyperfine and line width parameters are determined from fitting higher harmonics, the Lorentzian filter could be eliminated from the calculations producing a simulated spectrum that could be directly compared with the experimental first derivative EPR data. Fig. 4E shows a superposition of such spectra that were obtained without

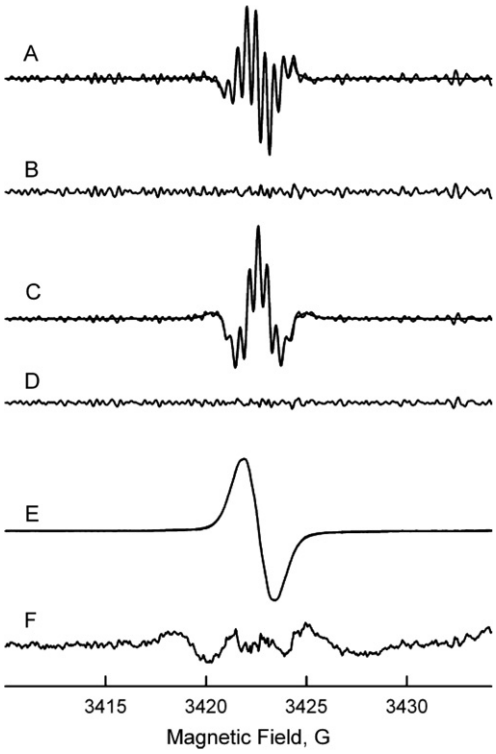

Fig. 4. Simultaneous least-squares simulations of the fifth (A) and the fourth (C) harmonics of the Cat1 EPR spectrum shown in Fig. 2A. Simulations are superimposed with the harmonics and residuals of the fitting—differences between the harmonics and the best fits—are depicted below each spectrum (B and D, respectively). (E) The superposition of the original Cat1 EPR spectrum with the best fit model constructed from fitting of higher harmonics and (F) the 20-fold magnified residual.

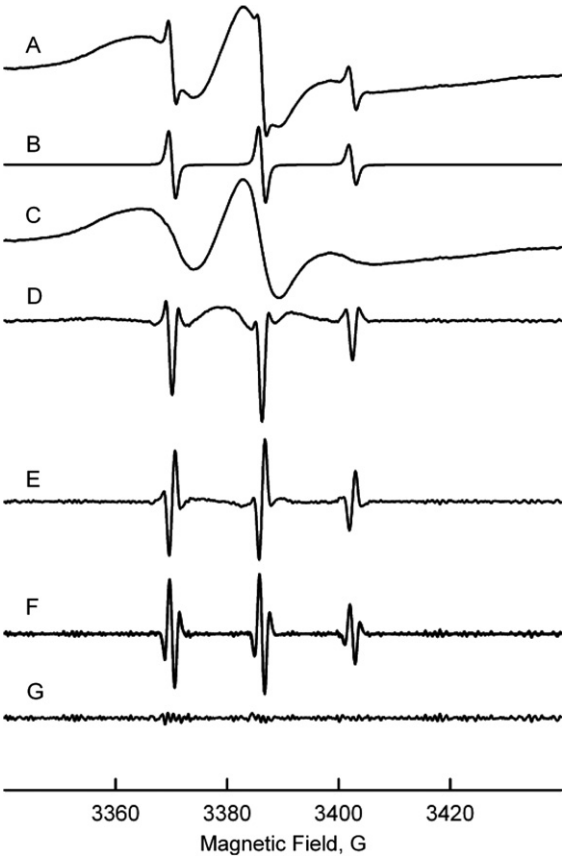

Fig. 5. (A) Experimental room temperature EPR spectrum from a spin-labeled peptide-16 of the transmembrane E2 glycoprotein of Sinbis virus reconstituted in 1:2 POPE/POPC lipid bilayers containing 30 mol% of cholesterol. Second (D), third (E), and fourth (F) harmonic displays show progressively enhanced contribution of fast-motion component. (G) The difference between the fourth harmonic and the least-squares model. (B and C) The reconstructed fast and slow components, respectively.

any parameter adjustments except minor correction of the signal phase. Because the fit and the experimental spectra were essentially undistinguishable, the residual of the fit was magnified 20-fold (Fig. 4F). This magnified residual reveals only minor deviations that are attributed to unaccounted ^{13}C satellite lines and a low field shoulder from the middle nitrogen hyperfine component. Notably, these broad features were effectively filtered out in the higher harmonics and were not noticeable.

Suppression of broad spectral components in the higher harmonic displays was found to be useful for separating spin-label EPR spectra arising from slow- and fast-motion components. This procedure is illustrated in Fig. 5 on an example of a room temperature spectrum of a peptide-16 (Ac-HHVYTILAVVTVAVLACAKKKKK-$CONH_2$) of the transmembrane E2 glycoprotein of Sinbis virus labeled at the unique cysteine with MTSL (1-oxyl-2,2,5,5-tetramethyl-3-pyrroline-3-methyl) and reconstituted in mixed POPE/POPC (1:2 molar ratio) lipid bilayers containing 30 mol% of cholesterol. Experimental X-band EPR spectrum (Fig. 5A, 2048 data points) has a sharp fast-motion component overlapping with the line that is tentatively attributed to an aggregated peptide. A sequence of higher harmonics has been generated using a Lorentzian filter with the peak-to-peak width of three data intervals (or 146 mG) for each of the consequent differentiation steps (D–F). While contributions from the broad lines are still noticeable in the second (D) and the third-derivative displays, the fourth derivative (F) contains mainly the fast-motion component. The latter spectrum was least-squares simulated according to an inhomogeneous line width model [12] and the results are superimposed with the fourth harmonic spectrum (F). The fit residual (G) shows only negligible deviations that are likely caused by approximating the unresolved proton hyperfine structure by a Gaussian envelope. The best-fit parameters were used to calculate the fast-motion component in the original first-derivative display (B) by simply eliminating the last step of convolution with the Lorentzian filter in the fourth harmonic form. Subtraction of the fast component (B) calculated this way yielded the broad component (C) without any apparent distortions.

4. Conclusion

It is shown that linear filtering of EPR spectra by digital convolution could be easily combined with other

post-processing manipulations such as calculations of higher harmonics and out-of-phase component. This is achieved by subjecting the filter function in the convolution equation to the differentiation and/or Kramers–Krönig operators. A particular emphasis was given to a Lorentzian filter that only adds homogeneous broadening to the spectral shapes. The broadening effect is additive for the Lorentzian function and, therefore, the spectral shape distortion caused by such a filtering could be easily and accurately accounted for in the consequent least-squares data modeling.

Multiple harmonic displays were found to be useful for determination of small hyperfine couplings that are otherwise hidden in poorly resolved experimental first derivative spectra. This could lead to elucidating detailed magnetic parameters of organic free radicals from conventional CW EPR without investing in additional hardware required for ENDOR and/or ESEEM experiments.

Another particularly attractive application of the convolution filtering method involves accurate separation of overlapping slow (broad) and fast (sharp) spectral components in spin-labeling EPR experiments. It is shown that the fast component could be digitally filtered out in a higher harmonic display, least-squares simulated to determine all the parameters, and precisely back-calculated as it would appear in the normal first-derivative display prior to any filtering.

It is worthwhile to note here that typical fitting of EPR spectra involves minimization of differences between the experimental $p(B)$ and the modeled spectra $m(B)$. While the approach presented here also relies on the least-squares minimization, the $(p(B) - m(B)) \otimes f(B)$ function is minimized instead of $(p(B) - m(B))$. The filter function $f(B)$ could be chosen to suppress undesirable contributions (such as, for example, broad spectral components as we demonstrated), or simply to change the weight of frequencies accounted for in the minimization. This fitting approach is not limited to the Lorentzian filter and could be worth of further exploration.

Acknowledgments

This work was supported by the DOE Contract DE-FG02-02ER15354 to A.S. (NCSU). The author is thankful to Drs. Smirnova and Rabah and Mr. Chadwick (NCSU) for providing experimental EPR spectra.

References

[1] J.S. Hyde, A. Jesmanowicz, J.J. Ratke, W.E. Antholine, Pseudomodulation: a computer-based strategy for resolution enhancement, J. Magn. Reson. 96 (1992) 1–13.

[2] J.S. Hyde, M. Pasenkiewich-Gierula, A. Jesmanowicz, W.E. Antholine, Pseudo field modulation in EPR spectroscopy, Appl. Magn. Reson. 1 (1990) 483–496.

[3] P.B. Sczaniecki, J.S. Hyde, W. Froncisz, Continuous wave multiquantum electron paramagnetic resonance spectroscopy. II. Spin-system generated intermodulation sidebands, J. Chem. Phys. 94 (1991) 5907–5916.

[4] M. Peric, M. Alves, B.L. Bales, Combining precision spin-probe partitioning with time-resolved fluorescence quenching to study micelles—application to micelles of pure lysomyristoyl-phosphatidylcholine (LMPC) and LMPC mixed with sodium dodecyl sulfate, Chem. Phys. Lipids 142 (2006) 1–13.

[5] T.I. Smirnova, T.G. Chadwick, M.A. Voinov, O. Poluektov, J. van Tol, A. Ozarowski, G. Schaaf, M.M. Ryan, V.A. Bankaitis, Local polarity and hydrogen bonding inside the sec14p phospholipid-binding cavity: high-field multi-frequency electron paramagnetic resonance studies, Biophys. J. 92 (2007) 3686–3695.

[6] B. Carlsson, M. Sternad, A. Ahlen, Digital differentiation of noisy data measured through a dynamic system, IEEE Trans. Signal Process. 40 (1992) 218–221.

[7] B.H. Robinson, C. Mailer, A.W. Reese, Linewidth analysis of spin labels in liquids. I. Theory and data analysis, J. Magn. Reson. 138 (1999) 199–209.

[8] B.H. Robinson, C. Mailer, A.W. Reese, Linewidth analysis of spin labels in liquids. II. Experimental, J. Magn. Reson. 138 (1999) 210–219.

[9] R.D. Nielsen, E.J. Hustedt, A.H. Beth, B.H. Robinson, Formulation of Zeeman modulation as a signal filter, J. Magn. Reson. 170 (2004) 345–371.

[10] C. Mailer, B.H. Robinson, B.B. Williams, H.J. Halpern, Spectral fitting: the extraction of crucial information from a spectrum and a spectral image, Magn. Reson. Med. 49 (2003) 1175–1180.

[11] Y. Deng, R.P. Pandian, R. Ahmad, P. Kuppusamy, J.L. Zweier, Application of magnetic field over-modulation for improved EPR linewidth measurements using probes with Lorentzian lineshape, J. Magn. Reson. 181 (2006) 254–261.

[12] A.I. Smirnov, R.L. Belford, Rapid quantitation from inhomogeneously broadened EPR spectra by a fast convolution algorithm, J. Magn. Reson. Ser. A 113 (1995) 65–73.

[13] R.N. Bracewell, Fourier Analysis and Imaging, Kluwer Academic/Plenum Publishers, New York, 2003.

[14] T.I. Smirnova, .A.I. Smirnov, R.B. Clarkson, R.L. Belford, W-band (95 GHz) EPR spectroscopy of nitroxide radicals with complex proton hyperfine structures: fast motion, J. Phys. Chem. 99 (1995) 9008–9016.

[15] A.I. Smirnov, R.B. Clarkson, R.L. Belford, EPR linewidth (T_2) method to measure oxygen permeability of phospholipid bilayers and its use to study the effects of low ethanol concentrations, J. Magn. Reson. B 111 (1996) 149–157.

[16] A.I. Smirnov, T.I. Smirnova, Convolution-based algorithm: from analysis of rotational dynamics to EPR oximetry and protein distance measurements, in: L.J. Berliner, C. Bender (Eds.), Biological Magnetic Resonance, vol. 21, Kluwer Academic, New York, 2004, pp. 277–348.

[17] T.I. Smirnova, A.I. Smirnov, S. Pachtchenko, O.G. Poluektov, J. Am. Chem. Soc. 129 (2007) 3476–3477.

[18] B. Kirste, A. Krueger, H. Kurreck, ESR and ENDOR investigations of spin exchange in mixed galvinoxyl/nitroxide biradicals. Syntheses, J. Am. Chem. Soc. 104 (1982) 3850–3858.

[19] K.K. Fox, Isotropic proton hyperfine coupling constants of two cationic nitroxides, J. Chem. Soc. Faraday Trans. 2 (1976) 975–983.